Momentum filter using resonant Zener tunneling

I. Kyriakou,[1,2] J. H. Jefferson,[1] G. Giavaras,[1,2,*] M. Fearn,[1] and C. J. Lambert[2]
[1]*QinetiQ, St. Andrews Road, Malvern WR143PS, England*
[2]*Department of Physics, Lancaster University, Lancaster LA14YB, England*
(Received 15 November 2006; revised manuscript received 16 April 2007; published 16 July 2007)

We consider the formation of a double barrier structure which includes both the valence and conduction bands in an InSb/InAlSb quantum well system and demonstrate basic features of the transport process through this structure, which exhibits Zener tunneling. In particular, we employ an eight-band model and the Landauer-Büttiker formalism [Phys. Rev. B **31**, 6207 (1985)] to investigate the transport process which under high confinement involves resonant energy levels due to the induced quasibound states in the valence bands. The mechanism of momentum filtering, taking advantage of resonant Zener tunneling, is shown to give improved performance at elevated temperatures compared with a unipolar double barrier resonant tunneling structure.

DOI: 10.1103/PhysRevB.76.045316 PACS number(s): 73.23.−b, 73.63.Hs, 73.63.Nm

I. INTRODUCTION

The Zener tunneling mechanism,[1] which involves interband tunneling through the energy gap of the corresponding material, i.e., tunneling from the conduction band into the valence bands and vice versa, has been well studied for bulk semiconductors[2–5] and observed, for example, in heavily doped *p-n* diode structures under a high reverse bias voltage.[4,5] One interesting consequence of the tunneling process is the increase of the current as a function of reverse bias up to the breakdown condition, a feature that makes tunnel diodes attractive in solid state devices for achieving fast switching times and fabricating low-power electronics.[6–8] Tunnel diodes also give rise to so-called negative differential resistance,[9,10] an effect which is revealed in the current versus applied voltage diagram and is widely studied and employed in nanostructures.[11–13]

As has been demonstrated, Zener interband tunneling can also be induced in a two-dimensional electron gas (2DEG) system[14,15] for electric fields of order MV/cm and the appropriate band bending conditions which are achieved via band engineering. The more complicated resonant Zener tunneling mechanism has been studied theoretically in *p-i-n* diodes[16] and demonstrated experimentally by Morifuji *et al.*[17]

In this work, we deal with the so-called Zener double barrier structure[18] (ZDBS) which involves resonant Zener tunneling and can be formed in a narrow gap quantum well material due to a well-localized high electric field from a surface gate. We use an eight-band model and the Landauer-Büttiker formalism in order to demonstrate a momentum filter based on resonant Zener tunneling and compare the mechanism with that in a conventional unipolar double barrier structure (DBS).[19,20] The efficiency of the ZDBS suggests that we can use this system to probe Zener properties in surface gated narrow gap 2DEG systems up to room temperature.

This paper is organized as follows. In Sec. II, we describe an appropriate device geometry and the basic model. In Sec. III, we present the main results, and Sec. IV summarizes the work.

II. DEVICE GEOMETRY AND BASIC MODEL

A. Zener double barrier structure

A possible device geometry to form a ZDBS is shown schematically in Fig. 1(a). The gates G_1 and G_2 on the surface of a quantum well structure control the transverse confinement in the plane of the 2DEG, whereas the additional gate G_3 controls the confinement along the transport direction z. Back gates can also be used for a more efficient control of the potential landscape.[21,22] For a narrow gap quantum well structure such as $InSb/In_{1-x}Al_xSb$, considered in this work, and sufficiently high electric field, the potential profile along z is shown in Fig. 1(b). This simplified picture of the band diagram shows that the ZDBS involves well-separated discrete energy levels in the valence band due to the induced confinement in all three spatial dimensions. These quantized levels arise from the heavy and light hole bands with the former being much more closely spaced due to the higher mass. In particular, confined energy levels in the valence band above the asymptotic conduction band edge have quasibound character and give rise to resonant Zener tunneling in and out of the confined region under gate G_3.

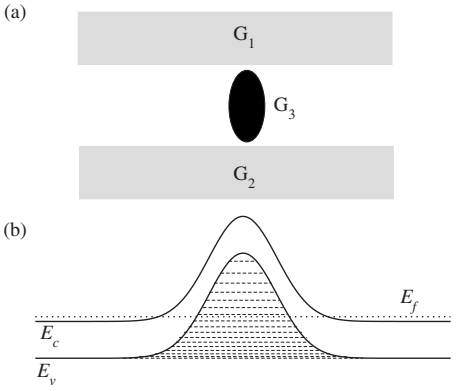

FIG. 1. (a) Schematic illustration of a possible gate design to induce the ZDBS. The gates G_1 and G_2 control transverse confinement in the plane of the 2DEG and the gate G_3 controls confinement along the transport z direction. (b) Simplified schematic illustration of the potential landscape of the ZDBS in the plane of the 2DEG and along the transport direction (for a detailed description of the band structure, see the text). The solid lines represent conduction (E_c) and valence band (E_v) edges. The dotted line indicates the Fermi energy (E_F), and the dashed lines indicate quantized energy levels in the valence band due to the strong confinement. The energy levels above the conduction band edge, which correspond to quasibound states, allow resonant Zener tunneling.

Since the aim of this work is to demonstrate theoretically the mechanism of momentum filtering using resonant Zener tunneling in an InSb/$In_{1-x}Al_xSb$ quantum well, without trying to model specific experimental devices, we have assumed for simplicity a constant potential in confinement regions and a linear approximation to the potential shown schematically in Fig. 1(b) along the transport direction. Specifically, for our work the ZDBS potential landscape along z is modeled using a linear potential approximation, i.e., $V(z)=-(V_o/L)|z|+V_o$, $(V_o>0)$ when $-L\leqslant z\leqslant L$ and $V(z)=0$ otherwise, which results in a constant electric field of magnitude $\mathcal{E}=V_o/L$. We note that a more accurate self-consistent calculation in all three spatial dimensions, which takes into account the hole charge in the valence bands, would change the position of the resonances; however, the main mechanism that we describe below would still be efficient provided the gate bias is adjusted to maximize the transmitted current according to the resulting position of the resonances.

The resonant tunneling mechanism through the ZDBS is analogous to that occurring in a unipolar DBS, which is the fundamental element in a resonant tunneling diode.[19,20] This is because an electron in the conduction band will tunnel through the classically forbidden regions that act as barriers. The barrier thickness depends on the value of the energy gap and the gate-induced electric field. To be specific, the effective Zener barriers become narrower with increasing electric field and decreasing energy gap. In addition, when the confinement is strong between the barriers, i.e., in the valence band, resonant tunneling can take place due to the appearance of quasibound states, leading to perfect transmission on resonance. This two-step process includes tunneling from the conduction to the valence bands and vice versa. By contrast, in the DBS we are dealing with resonant tunneling through barriers within the same band. For this reason, the theoretical approach for the ZDBS requires a multiband model which we describe below.

B. Band structure model

The structures of the bound and quasibound states under gate G_3 in Fig. 1 involve both light and heavy holes. Kane's eight-band model[23–25] includes these bands and in the bulk they may be decoupled, separating the heavy hole band from the coupled conduction and light hole valence bands (two-band model), with the split-off band somewhat lower in energy. For the ZDBS problem, this approach is inadequate in two respects. Firstly, because of lateral confinement (due to the quantum well confinement in the x direction and gates G_1 and G_2 in the y direction), decoupling of the eight-band model is no longer possible. Secondly, the mass of the heavy holes determines the number and properties of the resonances, and Kane's approximation (which does not include the dispersion of the heavy holes) is not appropriate.

A more refined model that includes heavy hole dispersion and reproduces the correct effective mass has already been used in the literature for the description of GaAs/AlGaAs quantum wells using a $\mathbf{k}\cdot\mathbf{p}$ theory approach.[26,27] In fact, this model is based on some earlier work in which the extended eight-band Kane model was employed for calculations in a quantum well structure.[28] The approach of Schuurmans and co-workers[26–28] uses Kane's eight-band model and a basis set that takes the axis of angular momenta to be perpendicular to the z axis. It also includes the Dresselhaus[29] and the free electron terms. This is similar to Kane's original eight-band model but has the advantage that the five parameters it uses to describe the electron and hole states refer to effective masses that are more readily obtained for a specific material (in our case InSb). The resulting 8×8 Hamiltonian has the following form:

$$\begin{pmatrix} E_{cb} & -\sqrt{2}P_z & P_z & \sqrt{3}P_+ & 0 & -P_- & -\sqrt{2}P_- & 0 \\ & E_{lh} & G_1 & \sqrt{2}G_+ & -P_+^* & 0 & -\sqrt{3}G_- & G_2 \\ & & E_{so} & -G_+ & -\sqrt{2}P_+^* & \sqrt{3}G_- & 0 & \sqrt{2}G_2 \\ & & & E_{hh} & 0 & -G_2 & -\sqrt{2}G_2 & 0 \\ & & & & E_{cb} & \sqrt{2}P_z & -P_z & -\sqrt{3}P_- \\ & & & & & E_{lh} & G_1 & \sqrt{2}G_- \\ & & & & & & E_{so} & -G_- \\ & & & & & & & E_{hh} \end{pmatrix}, \tag{1}$$

where only the upper triangle of the Hermitian matrix is shown. This eight-band Hamiltonian together with the functional form of all the terms is described in detail in Ref. 27. The diagonal elements may be written as

$$E_{cb}=E_g+s\tilde{e},$$

$$E_{lh}=-\gamma_1\tilde{e}-\gamma_2\tilde{e}_1,$$

$$E_{so}=-\Delta-\gamma_1\tilde{e},$$

$$E_{hh}=-\gamma_1\tilde{e}+\gamma_2\tilde{e}_1,$$

where $E_g=0.24$ eV is the energy gap, $\Delta=0.81$ eV is the spin-orbit splitting in InSb, and s and $\gamma_{1,2}$ are dimensionless parameters that describe the coupling of the s, x, y, z states to

the other bands.[27] Their values are derived by the effective masses using the relationships

$$m_o/m_{hh} = \gamma_1 - 2\gamma_2,$$

$$m_o/m_{cb} = s + \lambda\left(1 + \frac{r}{2}\right),$$

$$m_o/m_{lh} = \gamma_1 + 2\gamma_2 + \lambda,$$

$$m_o/m_{so} = \gamma_1 + \frac{\lambda r}{2},$$

$$\lambda = \frac{4m_o P^2}{3\hbar^2 E_g},$$

$$r = \frac{E_g}{E_g + \Delta},$$

where m_o is the free electron mass and P is the Kane momentum matrix element $P = \sqrt{\frac{3}{2}}\hbar c$, with $c \simeq c_o/300$ and c_o the speed of light. For our work, the effective masses have the values[30] $m_{hh}=0.32m_o$, $m_{lh}=0.016m_o$, and $m_{cb}=0.014m_o$ for the heavy hole, light hole, and conduction band, respectively, which give $s=24.8$, $\gamma_1=10.9$, and $\gamma_2=3.9$. The energy terms $\tilde{e}$ and $\tilde{e}_1$ are

$$\tilde{e} = \frac{\hbar^2}{2m_o}(k_x^2 + k_y^2 + \tilde{k}_z^2),$$

$$\tilde{e}_1 = \frac{\hbar^2}{2m_o}(2\tilde{k}_z^2 - k_x^2 - k_y^2),$$

with $\tilde{k}_z = -i(\partial/\partial z)$. The transverse momenta k_x and k_y are given directly from the confinement in the x and y directions. For simplicity, we have modeled this by particle in a box standing waves with $k_x = n_x\pi/L_x$ and $k_y = n_y\pi/L_y$, where n_x, $n_y = 1, 2\ldots$ and L_x, L_y the corresponding widths in x and y directions, respectively. Note that for the calculations we add the potential term $V(z)$ of the ZDBS to the diagonal elements. Finally, the off-diagonal terms can be expressed as

$$P_z = \sqrt{\frac{1}{3}}(iP\tilde{k}_z + Bk_xk_y),$$

$$P_\pm = \sqrt{\frac{1}{6}}[iP(k_x \pm ik_y) + B\tilde{k}_z(k_y \pm ik_x)],$$

$$G_1 = \sqrt{2}\gamma_2\tilde{e}_1,$$

$$G_2 = -\sqrt{3}\gamma_2 e_2 + i2\sqrt{3}\gamma_3 k_x k_y,$$

$$G_\pm = \sqrt{6}\gamma_3\tilde{k}_z(k_x \pm ik_y).$$

The new dimensionless parameter γ_3 describes the anisotropy of the energy band structure around the Γ point when $\gamma_2 \neq \gamma_3$ and its value $\gamma_3=4.3$ follows from the relationship $m_o/m_{hh} = \gamma_1 - 2\gamma_3$ and $m_{hh}=0.44m_o$ (Ref. 30). These equations contain another energy term which is $e_2 = \hbar^2(k_x^2 - k_y^2)/2m_o$ and Kane's B parameter that describes the bulk inversion asymmetry splitting.[29] In our calculations, we set $B=0$ since we will not consider small spin-splitting effects. Note that the effective masses that are used for the calculation of $\gamma_{1,2,3}$ and s are independent of the value of B (Refs. 26 and 27). It should also be mentioned that the relationships between the $\gamma_{1,2,3}$ that this formalism uses and the Luttinger $\gamma_{1,L}$, $\gamma_{2,L}$ and $\gamma_{3,L}$ parameters[31] are $\gamma_{1,L} = \gamma_1 + \lambda/2$, $\gamma_{2,L} = \gamma_2 + \lambda/4$, and $\gamma_{3,L} = \gamma_3 + \lambda$, where λ is a dimensionless parameter whose exact expression is given in Ref. 27 and in our study was calculated to be $\lambda = 45.55$.

C. Transport model

Transport through the ZDBS is determined by solving the time-independent Schrödinger equation with Hamiltonian (1) as a scattering problem, in which incident electrons at the Fermi energy in the conduction band are transmitted or reflected. In these calculations, transmission in the z direction for each incident electron and allowed transverse mode (defined by n_x and n_y) is computed using a finite difference approximation to the eight-component Schrödinger equation.

In particular, we have adopted the scattering technique developed by Sanvito *et al.*,[32] which is based on the Landauer-Büttiker formalism,[33] to calculate conductance from transmission by summing over all modes. This numerical technique assumes an arbitrary scattering region attached to two semi-infinite crystalline leads and extracts all the relevant transport information assuming coherent propagation. The method is also easily extended to finite temperature calculations by integrating over a Fermi distribution in the leads as required in subsequent calculations. We also mention that our approach to calculate transmission amplitude for an incident energy is valid within the low-bias regime when the Landauer-Büttiker formalism is applicable.

As described in Ref. 32, the first main and general step involved in this method is the calculation of Green's function (GF) of an infinite lead and the application of boundary conditions to obtain the GF for the semi-infinite leads attached to the scattering region. The next step is the construction of an effective Hamiltonian H_{eff} taken from the scatterer Hamiltonian and its couplings to the leads by eliminating the degrees of freedom of the system with a method implemented by the Gaussian elimination.[34] The degrees of freedom of the our system are $8N$, where N are the mesh points in the transport direction. Because H_{eff} is energy dependent, we can calculate the GF of the system for each given energy. The total GF of the system is then calculated via Dyson's equation[32]

$$G(E) = [g^{-1}(E) - H_{eff}(E)]^{-1}, \quad (2)$$

where

$$g(E) = \begin{pmatrix} g_L(E) & 0 \\ 0 & g_R(E) \end{pmatrix}, \quad (3)$$

with g_L and g_R the GF of the left and the right lead, respectively. The total GF, in turn, allows the calculation of the scattering matrix (S matrix) that relates the outgoing wave amplitudes to the ingoing amplitudes at the leads, and thus the transmission and reflection probabilities. Finally, the conductance, considering the contribution from all open channels, is determined within the Landauer-Büttiker formalism by the expression $G=G_o\Sigma_n T_n$ with T_n the transmission probability of the nth channel and $G_o=2e^2/h$.

We point out that the Hamiltonian H of our scattering problem has to be separated into an intrapart H_o and an interpart H_1, i.e., $H=H_o+H_1$. This is because the z direction of transport is discretized so that for each mesh point we have an eight-band Hamiltonian (slice) in a particular potential value that appears in the diagonal terms. H_o is Hermitian and carries all the information about a particular mesh point and H_1 links H_o to the adjacent slices. Then the Schrödinger equation for the system can be written as

$$H_o|\psi(z)\rangle + H_1|\psi(z+1)\rangle + H_{-1}|\psi(z-1)\rangle = E|\psi(z)\rangle, \quad (4)$$

with $H_{-1}=H_1^\dagger$, E the corresponding incident energy, and $|\psi(z)\rangle$ a column vector which corresponds to the slice at the z position. Using Bloch's theorem, $|\psi(z)\rangle$ can be written as $|\psi(z)\rangle=e^{ik_z\cdot z}|k_z\rangle$ with $|k_z\rangle$ an eight-component column vector, corresponding to the degrees of freedom of each slice.

In our case, H_1 includes only the k_z-dependent terms of H and H_o the remaining elements that do not participate in the discretization. The energy terms that contain all k_x, k_y, $\tilde{k_z}$, are separated into two parts, which belong to H_o and to H_1. For example, the diagonal term

$$E_{cb} = E_g + s\frac{\hbar^2}{2m_o}(k_x^2 + k_y^2 + \tilde{k_z}^2) \quad (5)$$

is written as $E_{cb}=E_{cb,1}+E_{cb,o}$ with

$$E_{cb,1} = s\frac{\hbar^2}{2m_o}\tilde{k_z}^2, \quad E_{cb,o} = E_g + s\frac{\hbar^2}{2m_o}(k_x^2 + k_y^2). \quad (6)$$

Hence, the term $E_{cb,1}$ is the corresponding element of H_1 and the term $E_{cb,o}$ of H_o.

III. MOMENTUM FILTER MECHANISM

Before presenting results showing how the ZDBS can act as a momentum filter, we illustrate the behavior of the conductance for the simple case of very high confinement in the x and y directions such that only the lowest transverse mode is relevant (quantum wire). Figure 2 shows conductance in quantum units of $G_o=2e^2/h$ as a function of incident energy, which is measured relative to the conduction band edge, for temperature $T=0$ K and for an electric field of $\mathcal{E}=0.47$ MV/cm. The conductance displays resonances for some characteristic energies and increases smoothly close to unity with increasing energy. Analysis of the data reveals that the wide resonance, which occurs at energy $\sim$0.055 eV, arises from a light hole quasibound state, while the narrow

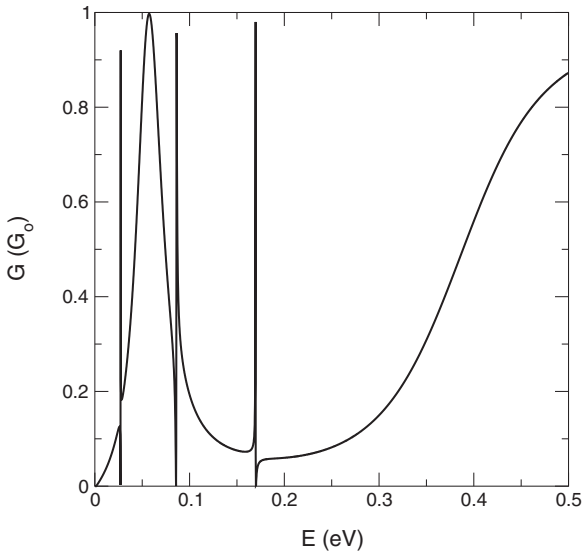

FIG. 2. Conductance (in units of $G_o=2e^2/h$) as a function of energy derived from the eight-band model, for an electric field of $\mathcal{E}=0.47$ MV/cm.

resonances are due to heavy hole states. The heavy hole resonances are relatively difficult to resolve requiring a very fine energy step and as a result, due to the numerical approach, yield a conductance slightly less than unity. An interesting feature is that the light hole resonance is much wider even than the heavy hole resonances that occur at higher energies because of the relative effective mass ratio. We also note that the split-off valence band does not generate resonances since it is $\sim$0.81 eV lower in energy than the heavy and light hole bands.

We can estimate the characteristic energies of the resonances by determining the bound energy states (E_n) of a one-dimensional quantum well that is identical to the Zener potential, since in the transport process these states have quasibound character allowing nearly perfect transmission. If we consider that the well is formed by an electric field $\mathcal{E}$, then for a particle of mass m^* the Wentzel-Kramers-Brillouin (WKB) approximation yields

$$E_n = \left[\frac{3\pi}{4}\left(n+\frac{1}{2}\right)\right]^{2/3}\left(\frac{e^2\hbar^2\mathcal{E}^2}{2m^*}\right)^{1/3}, \quad n=0,1,\ldots. \quad (7)$$

Using InSb parameters for the heavy and light hole masses and the electric field $\mathcal{E}=0.47$ MV/cm that we used before, we can determine to a good approximation the position of the resonances especially for the light hole band. Although such a check for the very narrow heavy hole resonances is not ideal, by shifting the corresponding heavy hole valence band edge we can monitor their number and position and thus verify their origin.

As it is well known from conventional p-n junctions, the tunneling process for a specific incident energy is efficient as long as the transverse momentum, controlled by k_x and k_y, is much smaller than the forward momentum k_z. In the ZDBS, the increase of transverse momentum lowers the conductance because it induces a larger effective band gap, leading to

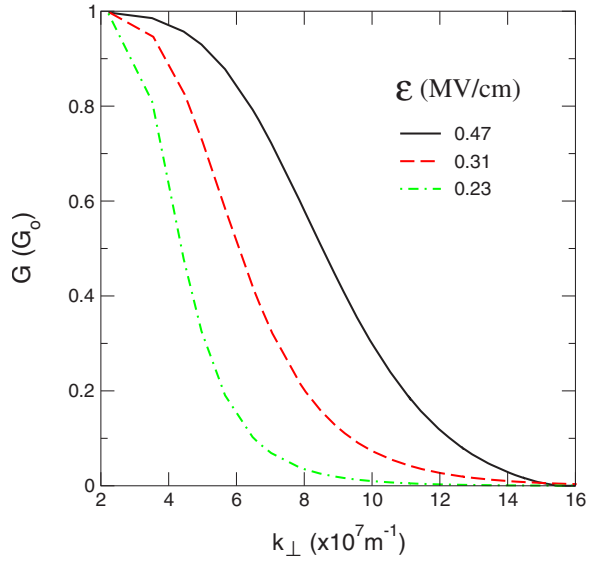

FIG. 3. (Color online) Conductance versus transverse momentum $k_\perp = k_\perp(n_x, n_y)$ for $T=0$ K and three different electric fields. These results are obtained from the eight-band model with Fermi energy fixed to give maximum conductance G_o for the lowest mode $n_x=n_y=1$ (light hole resonance).

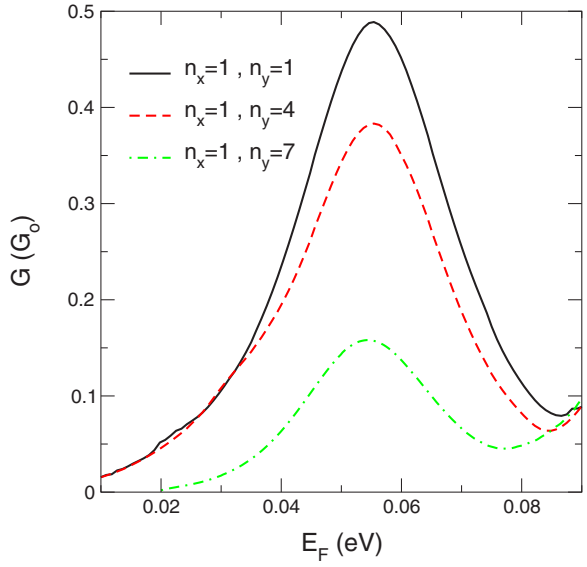

FIG. 4. (Color online) Conductance versus Fermi energy for the ZDBS at temperature $T=77$ K. Note that any extra resonances due to the heavy hole band are averaged out at finite temperatures. The curves correspond to different values of n_y, whereas in all cases $n_x=1$.

narrower resonances. Control of k_x and k_y can change the conductance drastically and this allows filtering of the momentum in the sense that the lower modes with larger forward component have the highest transmission probability close to resonance.

To analyze this behavior, we choose the transverse confinement lengths equal to $L_t=L_x=L_y=200$ nm (though the behavior is quite general) and perform transport calculations. For zero temperature, we set the Fermi energy of the system to yield maximum conductance for $n_x=n_y=1$ which comes from a light hole resonance and then calculate conductance for all the combinations of n_x and n_y of the allowed modes. As we see in Fig. 3, the conductance as a function of transverse momentum $k_\perp=\sqrt{k_x^2+k_y^2}=\pi\sqrt{n_x^2+n_y^2}/L_t$ maintains a relatively high value only for the few lowest modes for all the values of electric field, and drops to zero with increasing $k_\perp$. As in a unipolar DBS, the increase of transverse momentum leads to narrower conductance resonances which eventually become unresolvable at finite temperatures and the transmission is effectively blocked. Additionally, to understand the drop in conductance of the ZDBS, we need to consider that under strong transverse confinement the effective band gap increases, inducing stronger Zener barriers and thus lower tunneling probability. Note that this feature is not present in a DBS since the width of the rectangular barriers is fixed. We can see some of these effects by using the approximate quasirelativistic formula for the allowed miniband energies $E=\pm\sqrt{\frac{2}{3}P^2(k_\perp^2+k_z^2)+\left(\frac{E_g}{2}\right)^2}$ derived from the two-band model,[23] giving for $k_z\sim 0$ (conduction band edge) an effective energy gap of $\tilde{E}_g=2\sqrt{\frac{2}{3}P^2k_\perp^2+\left(\frac{E_g}{2}\right)^2}$, which increases with transverse momentum $k_\perp$. Since the $T=0$ K resonance widths have approximately an exponential decrease with effective band gap, as derived from a WKB approach,[18] the transmission through the higher transverse modes becomes too narrow to resolve, thus biasing the transmitted distribution to the forward direction. For example, with $L_x=L_y=200$ nm and $n_x=1$, the effective band gap almost doubles with $n_y\sim 9$ and the resonance width decreases 40 times. The modes n_x and n_y for which the resonances are too narrow to resolve depend, in general, on the well widths L_x and L_y and the Fermi energy. It is clear that if the well width is sufficiently small, the resonances will eventually not be resolved even for the second mode (i.e., $n_x=1$, $n_y=2$).

Another interesting feature shown in Fig. 3 is the strong dependence of the conductance on electric field. For example, an increase of the field from 0.23 to 0.47 MV/cm for a fixed incident energy leads to an increase of the conductance of nearly $0.8G_o$ units for $k_\perp\sim 6\times 10^7$ m^{-1}. This is because the increase in electric field results in broader resonances (due to the narrower Zener barriers), thus giving higher tunneling probability when we detune away from minimum $k_\perp$.

To extend the analysis to finite temperatures, we integrate over the Fermi distribution, giving the one-channel conductance[20] $G(E_F)=G_o\int T(E)F_T(E-E_F)dE$, where $F_T(E)$ is the thermal broadening function incorporating the Fermi-Dirac distribution in the leads. The value of the energy gap is given by the expression[30] $E_g(T)=E_g(0)-aT^2/(b+T)$, with $a=0.6$ meV K^{-1} and $b=500$ K, though this gap variation has a relatively small effect. In Figs. 4 and 5, we plot conductance versus Fermi energy for the ZDBS (for a field of $\mathcal{E}=0.47$ MV/cm) and the DBS, respectively, for a temperature of $T=77$ K and some combinations of transverse modes. It is important to observe that for a realistic comparison, the maximum value of conductance (for the lowest mode) has been chosen to be the same for both structures, i.e., $\sim 0.5G_o$, which arises from the ZDBS and DBS structures which have the same barrier width and height. In Fig. 4, the conductance

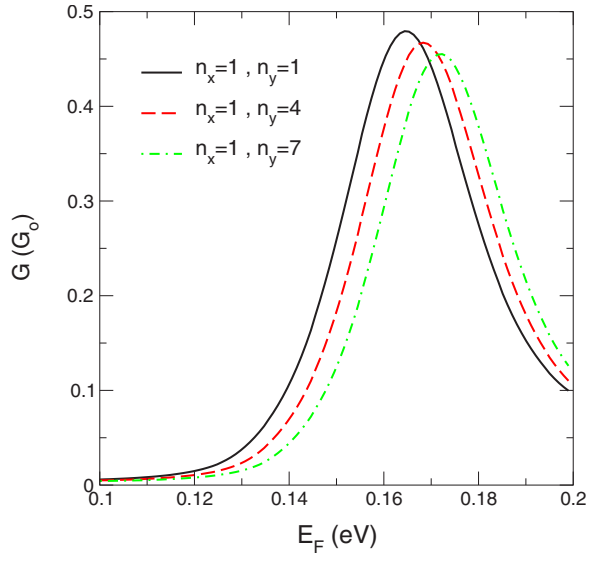

FIG. 5. (Color online) Conductance versus Fermi energy for the DBS at temperature $T=77$ K. For all the resonances, $n_x=1$ and different values of n_y are considered.

peak induced by a light hole resonance drops with increasing modes because, similar to the zero temperature case, the increased confinement leads to an increase of the effective band gap and hence narrower resonances. Note that at finite temperatures, the very sharp resonances due to the heavy holes are suppressed and no longer resolved. On the other hand, as shown clearly in Fig. 5 for the DBS, the increase of transverse confinement has a much weaker effect on the peak of the conductance since the resonance narrowing is much weaker.

By comparing Figs. 4 and 5, we demonstrate the improved efficiency of the ZDBS as a momentum filter compared to a DBS. For a more detailed description, we have performed calculations for a range of temperatures and determined the normalized quantity G/G_{lowest} as a function of transverse momentum $k_\perp$, with G_{lowest} the conductance of the lowest mode and E_F chosen such that G_{lowest} is maximum (light hole resonance). Figure 6(a) for the ZDBS for an electric field of $\mathcal{E}=0.47$ MV/cm shows a negligible dependence on temperature even at temperatures as high as $T=300$ K. This is because there is a significant drop in the height of the resonances as Fig. 4 shows, and as a result the thermal broadening at high temperatures has a small effect on the conductance. Note that we have also verified this behavior for other values of electric fields, within the order of MV/cm, which indicates that the ZDBS is robust to small changes of the induced potential. On the other hand, in the unipolar DBS for which results are shown in Fig. 6(b), the effect of broadening is clear and becomes much stronger with increasing temperature than that in the ZDBS. This is due to the fact that in the DBS, the increase of transverse confinement has a relatively small effect on the conductance as Fig. 5 indicates, simply because it results in transmission through slightly narrower quasibound states but not through substantially stronger tunnel barriers as in the ZDBS.

The conductance versus $k_\perp$ diagrams show that if L_x and L_y are small and very few modes are allowed, then there can be a situation in which only the lowest mode gives a nonnegligible contribution to the conductance. It is interesting to determine how small the wire width needs to be in order to give a momentum filter for which most of the transmitted electrons are in the lowest mode (maximum forward momentum). For an estimation, we choose $T=300$ K and determine the wire width which gives the very small value of $G/G_{lowest}\simeq 0.01$ for the second higher mode. In the ZDBS and for $\mathcal{E}=0.47$ MV/cm the wire width is ~ 45 nm, whereas for the DBS we calculate this width to be less than 10 nm, which shows clearly the potential advantages of a device based on Zener tunneling for momentum filtering.

IV. SUMMARY AND DISCUSSION

We have demonstrated a momentum filter using the ZDBS which includes both the conduction and valence bands of an InSb quantum well system. This structure can be

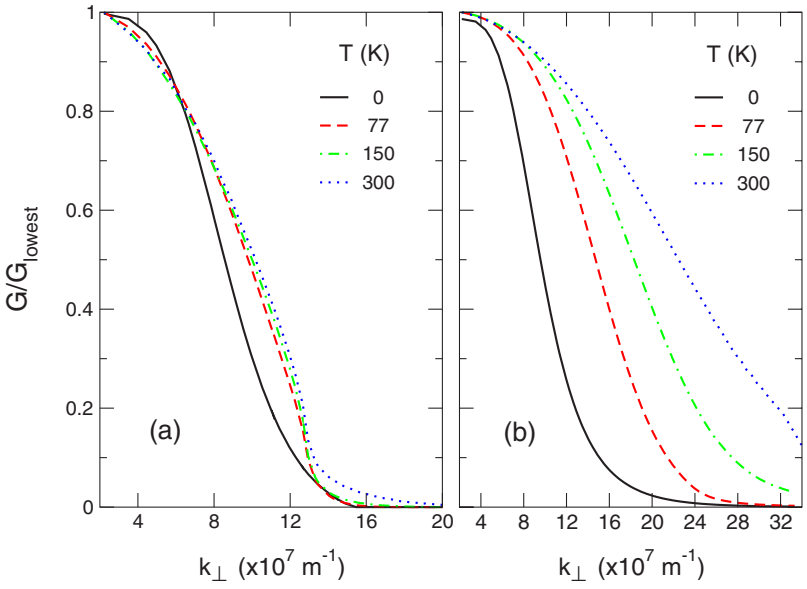

FIG. 6. (Color online) Dependence of normalized conductance G/G_{lowest} on transverse momentum $k_\perp$ in an InSb channel for various temperatures. Results for (a) the ZDBS for an electric field $\mathcal{E}=0.47$ MV/cm and (b) the unipolar DBS.

formed under a high electric field on the order of MV/cm due to a top gate voltage and leads to a band bending that allows Zener interband tunneling in a lateral configuration. The behavior of the conductance was investigated by employing a combination of an eight-band model[26–28] and the Landauer-Büttiker transport formalism.[33]

The conductance displays resonances due to heavy and light hole quasibound states whose width can be tuned with electric field, energy gap, temperature, and transverse momentum. With increasing transverse momentum or energy gap, or with decreasing electric field, the resonances become narrower and the conductance gradually drops to zero. In the opposite limits, nonresonant tunneling can take place and the conductance can have an appreciable value for a wide range of incident energies. The heavy hole resonances are difficult to resolve because of their very small width and for high temperatures $T > 77$ K they are almost totally suppressed. Hence, in the limit of high temperatures, the conductance peaks are only due to resonances resulting from the interaction between light hole and conduction bands.

The increase of the transverse momentum results in a significant drop in conductance for the ZDBS, because it gives rise to an enhanced narrowing of the quasibound states compared with an ordinary DBS. This is due to a larger effective band gap which leads to strong tunnel barriers between conduction and valence band states. We have shown how we can exploit the Zener resonant tunneling mechanism to filter momentum with only a few modes (the modes with the largest forward momentum) contributing to conductance, with Fermi energy chosen to give maximum conductance for the lowest allowed transverse momentum corresponding to a light hole resonance. Unlike in a DBS, in the ZDBS the conductance versus transverse momentum increases very little with increasing temperature, offering an efficient momentum filter in narrow gap 2DEG systems.

ACKNOWLEDGMENTS

Two of the authors (I.K. and G.G.) would like to thank U.K. EPSRC for funding. This work was supported by the U.K. Ministry of Defence.

*Present address: Department of Physics and Astronomy, University of Leicester, Leicester, England.

[1] C. Zener, Proc. R. Soc. London, Ser. A **145**, 523 (1934).
[2] S. M. Sze, *Physics of Semiconductor Devices*, 2nd ed. (Wiley, New York, 1981).
[3] C. B. Duke, *Tunneling in Solids* (Academic, New York, 1969).
[4] J. V. Morgan and E. O. Kane, Phys. Rev. Lett. **3**, 466 (1959).
[5] R. M. Minton and R. Glicksman, Solid-State Electron. **7**, 491 (1964).
[6] M. Sweeny and J. Xu, Appl. Phys. Lett. **54**, 546 (1989).
[7] R. Q. Yang, M. Sweeny, D. Day, and J. M. Xu, IEEE Trans. Electron Devices **38**, 442 (1991).
[8] T. C. L. G. Sollnerr, W. D. Goodhue, P. E. Tannenwald, C. D. Parker, and D. D. Peck, Appl. Phys. Lett. **43**, 588 (1983).
[9] L. Esaki, Phys. Rev. **109**, 603 (1958).
[10] L. L. Chang, L. Esaki, and R. Tsu, Appl. Phys. Lett. **24**, 593 (1974).
[11] J. Chen, M. A. Reed, A. M. Rawlett, and J. M. Tour, Science **286**, 1550 (1999).
[12] J. Chen, W. Wang, M. A. Reed, A. M. Rawlett, D. W. Price, and J. M. Tour, Appl. Phys. Lett. **77**, 1224 (2000).
[13] J. R. Söderström, D. H. Chow, and T. C. McGill, Appl. Phys. Lett. **55**, 1094 (1989).
[14] J. Allam, F. Beltram, F. Capasso, and A. Y. Cho, Appl. Phys. Lett. **51**, 575 (1987).
[15] J. P. Eisenstein, L. N. Pfeiffer, and K. W. West, Appl. Phys. Lett. **58**, 1497 (1991).
[16] A. Di Carlo, P. Vogl, and W. Pötz, Phys. Rev. B **50**, 8358 (1994).
[17] M. Morifuji, T. Imai, C. Hamaguchi, A. Di Carlo, P. Vogl, G. Böhm, G. Tränkle, and G. Weimann, Phys. Rev. B **65**, 233308 (2002).
[18] D. Gunlycke, J. H. Jefferson, S. W. D. Bailey, C. J. Lambert, D. G. Pettifor, and G. A. D. Briggs, J. Phys.: Condens. Matter **18**, S843 (2006).
[19] N. C. Kluksdahl, A. M. Kriman, D. K. Ferry, and C. Ringhofer, Phys. Rev. B **39**, 7720 (1989).
[20] S. Datta, *Electronic Transport in Mesoscopic Systems* (Cambridge University Press, Cambridge, New York, 1995).
[21] G. Borgioli, G. Frosali, and P. F. Zweifel, Transp. Theory Stat. Phys. **32**, 347 (2003).
[22] G. Bastard, *Wave Mechanics Applied to Semiconductor Heterostructures* (Les Éditions de Physique, Les Ulis, 1988).
[23] E. O. Kane, J. Phys. Chem. Solids **1**, 249 (1957).
[24] E. O. Kane in *Narrow Gap Semiconductors: Physics and Applications*, edited by W. Zawadzki, Lecture Notes in Physics Vol. 133 (Springer Verlag, Berlin, 1980).
[25] E. O. Kane, *Physics of III–V Compounds* (Academic, New York, 1966), Vol. 1, Chap. 3.
[26] R. Eppenga and M. F. H. Schuurmans, Phys. Rev. B **37**, 10923 (1988).
[27] R. Eppenga, M. F. H. Schuurmans, and S. Colak, Phys. Rev. B **36**, 1554 (1987).
[28] M. F. H. Schuurmans and G. W.'t Hooft, Phys. Rev. B **31**, 8041 (1985).
[29] G. Dresselhaus, A. F. Kip, and C. Kittel, Phys. Rev. **98**, 368 (1955).
[30] *Landolt-Börnstein, Numerical Data and Functional Relationships in Science and Technology, New Series*, Group III. Solid State Physics (Springer-Verlag, Berlin, 1997).
[31] J. M. Luttinger, Phys. Rev. **102**, 1030 (1956).
[32] S. Sanvito, C. J. Lambert, J. H. Jefferson, and A. M. Bratkovsky, Phys. Rev. B **59**, 11936 (1999).
[33] M. Büttiker, Y. Imry, R. Landauer, and S. Pinhas, Phys. Rev. B **31**, 6207 (1985).
[34] C. J. Lambert, V. C. Hui, and S. J. Robinson, J. Phys.: Condens. Matter **5**, 4187 (1993).